12 February 1999

Chemical Physics Letters 300 (1999) 651–655

CHEMICAL PHYSICS LETTERS

Construction of simple gold nanoparticle aggregates with controlled plasmon–plasmon interactions

Sarah L. Westcott [a], Steven J. Oldenburg [a], T. Randall Lee [b], Naomi J. Halas [a,*]

[a] Department of Electrical and Computer Engineering and the Rice Quantum Institute, Rice University, Houston, TX 77005, USA

[b] Department of Chemistry, University of Houston, Houston, TX 77204, USA

Received 23 September 1998; in final form 23 November 1998

Abstract

We have developed a colloidal assembly for the study of plasmon–plasmon interactions between gold nanoparticles. Colloidal aggregates of controlled size and interparticle spacing were synthesized on silica nanoparticle substrates. Following the immobilization of isolated gold nanoparticles onto silica nanoparticles, the surfaces of the adsorbed gold nanoparticles were functionalized with 4-aminobenzenethiol. This molecular linker attached additional gold nanoparticles to the 'parent' gold nanoparticle, forming small nanoparticle aggregates. The optical absorption spectrum of these clusters differed from that of gold colloid in a manner consistent with plasmon–plasmon interactions between the gold nanoparticles.

The self-assembly of nanoparticles into dense arrays, crystals, and Langmuir–Blodgett films yields materials with novel physical properties arising from interactions between nanoparticles [1–3]. Particle–particle interactions also regulate the linear and nonlinear optical properties of nanoparticles embedded in matrices or assembled into thin films at a high volume fraction [4,5]. Currently, there is great motivation to exploit the unique properties of these materials in electronic and optical device applications.

Whereas attention is focussed primarily on the assembly of macroscopic crystals and films of dense cluster matter, there is also interest in developing methods for assembling small controlled aggregates of nanoparticles, or 'artificial molecules'. Due to the spherical symmetry and uniform reactivity of individual nanoparticle surfaces, the synthesis of small controlled nanoparticle assemblies is a significant challenge. Recently, however, DNA was utilized to provide the necessary symmetry-breaking mechanism to synthesize nanoparticle dimers [6].

In this Letter, we report the stepwise molecular assembly of small, controlled aggregates of gold nanoparticles. Silica nanoparticles were used as substrates to provide the symmetry-breaking mechanism necessary for controlled assembly of these small gold nanoparticle aggregates. This approach provided hundreds of cm^2 of silica surface area per milliliter of solution, facilitating the observation of

* Corresponding author. E-mail: halas@faraday.rice.edu

PII: S0009-2614(98)01410-9

the optical properties of the assembled aggregates. The distance between aggregated gold nanoparticles was primarily controlled by a molecular linker, which covalently attached the constituent nanoparticles to each other [7]. Short molecular linkers were used so that the interparticle spacing would be small compared to the mean nanoparticle radius. Established theoretical descriptions of Mie scattering from similar small aggregate clusters [8,9] suggested that the plasmon resonance absorption of the aggregates would have an additional long wavelength component in the optical absorption spectrum relative to the absorption from isolated nanoparticles dispersed in solution. This component arises from the interactions of the plasmon resonances of the individual gold nanoparticles. The growth scenario for these aggregates is quite different from the recently reported adsorption of colloidal aggregates formed in solution onto silica nanoparticle surfaces in certain solvent mixtures [10].

The silica nanoparticle substrates used in this experiment were grown using the Stöber method [11]. Nanoparticles of nominally 125 nm diameter were used. The surfaces of these nanoparticles were functionalized with a mixture of 2% 3-aminopropyltrimethoxysilane (APTMS) and 98% *n*-propyltrimethoxysilane (PTMS) [12]. This mixture yielded silica nanoparticles whose surfaces were terminated with amine groups in dilute coverage dispersed among propyl groups. Gold nanoparticles of nominally 8 nm diameter were grown from smaller gold nanoparticles and stabilized with sodium citrate [13]. Since gold nanoparticles can be bound to substrates via amine groups [13], mixing the gold nanoparticles with the functionalized silica nanoparticles resulted in immobilization of a dilute coverage of gold nanoparticles onto the silica nanoparticle surfaces [14]. Excess gold nanoparticles were removed from solution by repeated cycles of centrifuging and redispersing in 0.4 mM aqueous sodium citrate (at least four repetitions). A JEOL JEM-2010 transmission electron microscope (TEM) was used to image representative nanoparticle structures at various stages of the assembly process. In Fig. 1a, a TEM image of the immobilized gold nanoparticles on a silica nanoparticle is shown. The UV–visible extinction spectrum of this solution, displayed in Fig. 2a, shows a strong absorption at 516 nm due to the plasmon resonance absorption of the gold nanoparticles. The immobilized gold nanoparticles typically covered only about 15% of the surface area of the silica nanoparticles when prepared in this manner.

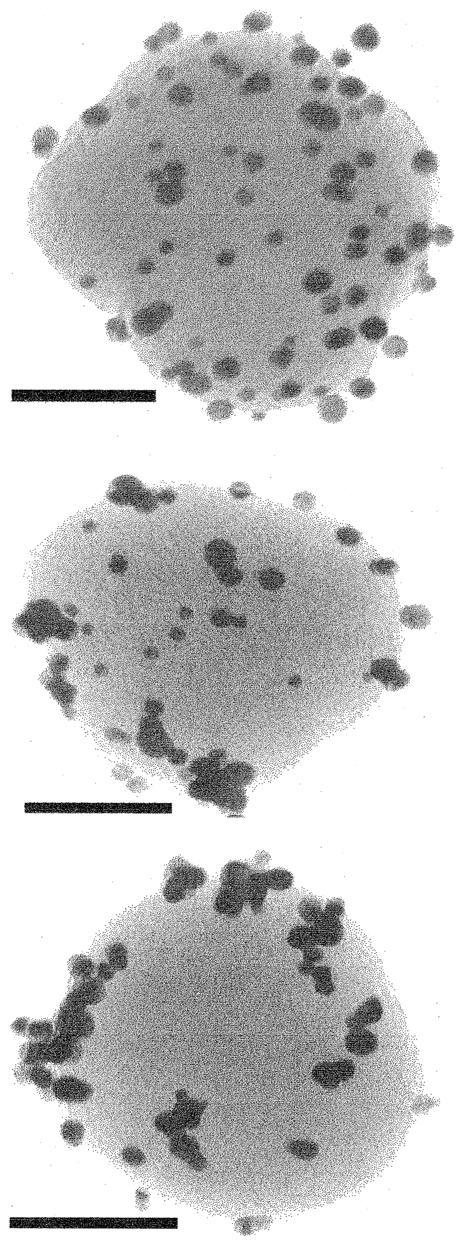

Fig. 1. (a) TEM image of the initial layer of gold nanoparticles adsorbed on the functionalized silica nanoparticles. (b) TEM image of the bound gold nanoparticles after adding 4-aminobenzenethiol to the solution. (c) TEM image of linked gold nanoparticles. All scale bars are 50 nm.

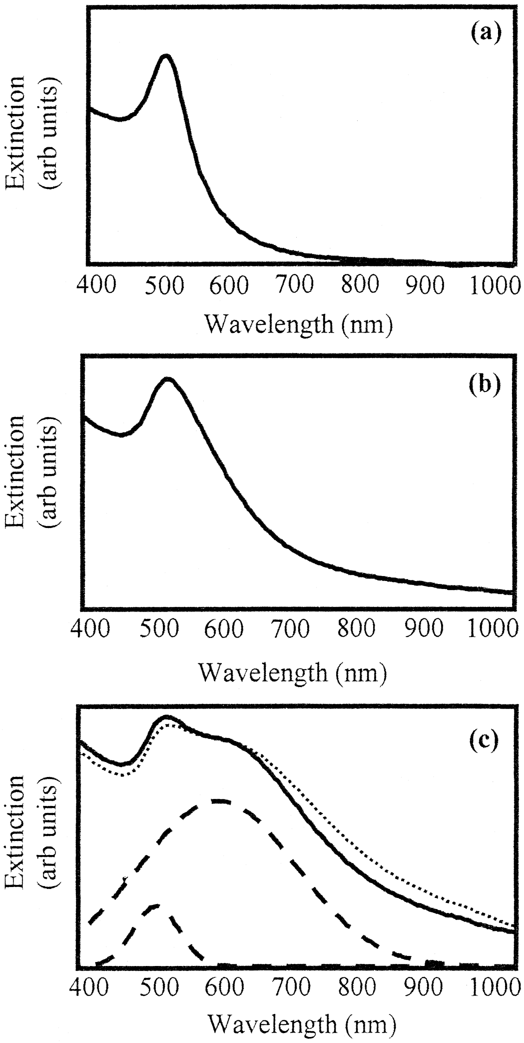

Fig. 2. (a) UV–visible extinction spectrum of gold nanoparticles bound on the surfaces of silica nanoparticles. (b) UV–visible extinction spectrum after binding 4-aminobenzenethiol to the adsorbed gold nanoparticles. (c) UV–visible extinction spectrum of the aggregates of gold nanoparticles on the silica nanoparticles' surfaces (solid line). The dashed lines are Gaussian fits to the two peaks and the dotted line is the UV–visible extinction spectrum of the aggregates taken 10 weeks after the nanostructures were prepared.

The bifunctional molecule 4-aminobenzenethiol can attach to the surface of gold nanoparticles via either its amine or thiol functional group. Upon addition of 4-aminobenzenethiol to a solution of the 'gold-decorated' silica nanoparticles, one functional group reacted with the immobilized gold nanoparticles while the other functional group was extended outward from the nanoparticles (due necessarily to the rigid nature of the intervening aromatic moiety). Fig. 1b and Fig. 2b show a TEM image of a representative nanoparticle and a corresponding UV–visible spectrum after the addition of 4-aminobenzenethiol. In the TEM image, it seems that some gold nanoparticles associated when the 4-aminobenzenethiol was added, suggesting the gold nanoparticles had at least limited mobility on the silica nanoparticle surface. The maximum in the UV–visible spectrum shifts from 516 to 527 nm and broadens slightly. Association of a small number of nanoparticles would give rise to such a shift and might be responsible for the broadening. The shift might also arise from the change in the dielectric constant of the local embedding medium due to the adsorbed 4-aminobenzenethiol molecules [15].

After centrifuging and redispersing several times to remove any excess linker molecule, additional gold nanoparticles were added to the solution. These gold nanoparticles were allowed to react with the extended functional group, generating structures in which gold nanoparticles were attached to each other via the rigid molecular linker. TEM images show that structures of linked gold nanoparticles were prevalent (Fig. 1c). Compared to the previous optical absorption spectra (Fig. 2a,b), the spectrum of the solution containing the linked nanostructures exhibited a markedly different appearance (Fig. 2c). This double-peaked spectrum consists of two broad resonances with maxima at 513 nm and 604 nm (dashed lines). The emergence of the long wavelength peak is consistent with predicted modifications in the optical spectrum due to plasmon–plasmon interactions between the gold nanoparticles [8,9]. The second peak is relatively broad because its position is dependent on both the number of coupled nanoparticles and their relative position with respect to each other and to the incident light.

Examination of the number of nanoparticles in each aggregate in the TEM images revealed two size regimes of aggregates. First, there were aggregates consisting of a small number of nanoparticles characterized by the distribution shown in Fig. 3. The majority of these small aggregates had only two nanoparticles. There were also larger aggregates

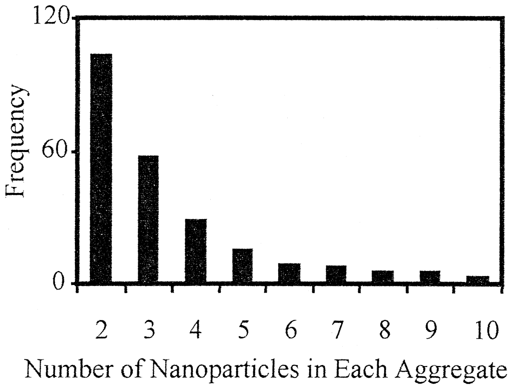

Fig. 3. Histogram showing the distribution of the number of gold nanoparticles in each small aggregate.

where the exact number of nanoparticles was difficult to evaluate, which consisted of approximately 15–50 nanoparticles per aggregate. An example of a larger aggregate can be seen on the left side of the TEM image in Fig. 1c. These larger aggregates might have formed through the merging of smaller neighboring aggregates immobilized on the silica nanoparticle surface. Of the total number of gold nanoparticles, about half existed in small aggregates; the other half were in large aggregate clusters.

The final assembled nanostructures were remarkably stable. After 2 weeks, the observed UV–visible absorption spectrum was only slightly broadened. The spectrum showed no further change over another 8 weeks (Fig. 2c, dotted line). By comparison, when 4-aminobenzenethiol was added directly to a solution of gold nanoparticles, the nanoparticles flocculated rapidly and could not be redispersed.

Although exposure of gold nanoparticles to silica nanoparticles functionalized with 100% APTMS led to higher initial coverage of gold nanoparticles, the coverage was still limited to $\sim 25\%$ due to electrostatic repulsion between the nanoparticles [16]. Further treatment of these nanoparticles with 4-aminobenzenethiol followed by additional gold nanoparticles yielded mostly larger aggregate structures. The UV–visible extinction spectra showed a double-peaked structure with a broader, less distinct high wavelength peak.

Since the initial layer of gold nanoparticles covered no more than 25% of the surface area of the silica nanoparticles, there were likely to be unreacted amine groups on the silica nanoparticle surface after the first addition of gold nanoparticles. These excess amine groups might have been able to provide attachment sites upon addition of the second portion of gold nanoparticles. To test the reactivity of these excess amine groups, we attached a layer of small (2 or 3 nm diameter) gold nanoparticles onto 100% APTMS-functionalized silica nanoparticles (surface area coverage $< 30\%$). This solution was then divided into three batches. One was reacted with 4-aminobenzenethiol, another with 2-aminoethanethiol, and the last with no linker molecule. When a solution of large (8 nm) gold nanoparticles was added, at least 30 large gold nanoparticles attached to each silica nanoparticle in the batches that had been reacted with 4-aminobenzenethiol or 2-aminoethanethiol. For the batch without a linker molecule, at least 85% of the silica nanoparticles had no large gold nanoparticles and the remainder of the silica nanoparticles had fewer than 10 large gold nanoparticles each. We thus conclude that the predominant linking mechanism for the gold nanoparticles involves the bifunctional linker rather than the excess amine groups on the silica nanoparticle surface.

Another concern was that the molecules might simply be reducing the surface charge of the gold nanoparticles by replacing the citrate ions. During experiments involving the adsorption of gold nanoparticles on planar substrates, molecular adsorption was used to reduce the electrostatic repulsion between nanoparticles and allow more gold nanoparticles to react with the functionalized surface [16]. To test this possibility, we prepared a solution of immobilized large gold nanoparticles, added *n*-propylamine (which possesses only one functional group that can bind to gold nanoparticles), and then added more large gold nanoparticles. Analysis by TEM showed no change in coverage of gold nanoparticles; there was also no change in the optical properties. These results thus provide further support for the participation of the linker molecules in the attachment process.

Although the 2-aminoethanethiol was a successful linker molecule for attaching large (~ 8 nm) gold nanoparticles to small (~ 2 nm) immobilized gold nanoparticles, it could not be used to attach large gold nanoparticles to large immobilized gold nanoparticles. Attachment attempts resulted in the removal of the immobilized large gold nanoparticles from the silica nanoparticles and the formation of extensive fractal-type linked structures of gold nanoparticles in solution upon the addition of the second portion of gold nanoparticles. At present, we cannot distinguish whether differences in molecular rigidity or acid-base properties are responsible for the different linking abilities of 2-aminoethanethiol and 4-aminobenzenethiol.

In summary, we have demonstrated a procedure for synthesizing small, controlled aggregates of gold colloid using molecular linkers and nanoparticle substrates. The bifunctional linker molecules position the colloidal nanoparticles in close proximity to each other, causing a modification in their optical properties due to plasmon–plasmon interactions. This new approach to preparing small cluster aggregates of controlled particle size and optical characteristics might prove valuable in applications such as surface enhanced Raman scattering (SERS) or chemical sensing.

Acknowledgements

Research was supported by the Robert A. Welch Foundation, the National Science Foundation, The Office of Naval Research and NASA. SLW acknowledges NSERC for fellowship support.

References

[1] R.P. Andres, J.D. Bielefeld, J.I. Henderson, D.B. Janes, V.R. Kolagunta, C.P. Kubiak, W.J. Mahoney, R.G. Osifchin, Science 273 (1996) 1690.
[2] C.B. Murray, C.R. Kagan, M.G. Bawendi, Science 270 (1995) 1335.
[3] C.P. Collier, R.J. Saykally, J.J. Shiang, S.E. Henrichs, J.R. Heath, Science 277 (1997) 1978.
[4] M.J. Feldstein, C.D. Keating, Y.-H. Liau, M.J. Natan, N.F. Scherer, J. Am. Chem. Soc. 119 (1997) 6638.
[5] Z. Liu, H. Wang, H. Li, X. Wang, Appl. Phys. Lett. 72 (1998) 1823.
[6] A.P. Alivisatos, K.P. Johnsson, X. Peng, T.E. Wilson, C.J. Loweth, M.P. Bruchez Jr., P.G. Schultz, Nature 382 (1996) 609.
[7] T. Sato, H. Ahmed, D. Brown, B.F.G. Johnson, J. Appl. Phys. 82 (1997) 696.
[8] U. Kreibig, M. Vollmer, Optical Properties of Metal Clusters, Springer, New York, 1995.
[9] M. Quinten, U. Kreibig, Surf. Sci. 172 (1986) 557.
[10] S.L. Westcott, S.J. Oldenburg, T.R. Lee, N.J. Halas, Langmuir 14 (1998) 5396.
[11] W. Stöber, A. Fink, E. Bohn, J. Colloid Interface Sci. 26 (1968) 62.
[12] A. van Blaaderen, A. Vrij, J. Colloid Interface Sci. 156 (1993) 1.
[13] K.C. Grabar, K.J. Allison, B.E. Baker, R.M. Bright, K.R. Brown, R.G. Freeman, A.P. Fox, C.D. Keating, M.D. Musick, M.J. Natan, Langmuir 12 (1996) 2353.
[14] S.J. Oldenburg, R.D. Averitt, S.L. Westcott, N.J. Halas, Chem. Phys. Lett. 288 (1998) 243.
[15] S. Underwood, P. Mulvaney, Langmuir 10 (1994) 3427.
[16] K.C. Grabar, P.C. Smith, M.D. Musick, J.A. Davis, D.G. Walter, M.A. Jackson, A.P. Guthrie, M.J. Natan, J. Am. Chem. Soc. 118 (1996) 1148.